Article can be accessed online at http://www.publishingindia.com

Combining Bilateral Filtering and Fusion of Visual and IR Images

Shanmugasundaram Marappan*

Abstract

This paper presents efficient fusion algorithms to discover hidden objects in the visual scene bymeans of merging visual and infrared images of the same scene. Generally, images are corrupted by noise. It is highly difficult to discover the objects in the corrupted image due to different types of noise appearing in the images. To remove noise while preserving edges in noisy input images, bilateral filter is proposedin this paper. Most popular fusion techniques including average and condition rule is employed to obtain a complement fused image from the noisy source images. Along with these two fusion rules, four algorithms have been generated with bilateral filter for finding hidden objects. First, the visual and IR sources degraded by noise are smoothed by bilateral filter. Second, both IR and visual-denoised images are fused by applying one of the proposed pixel-level techniques. The proposed algorithms are tested over four sets of visual and IR images to find out objects that are having worse background as smoke, illumination and bad weather climate. Experiments have been carried out and results were obtained.

Keyword: Image Fusion, Bilateral Filter, Object Detection, Hidden Objects, IR Image, Multisensor

Introduction

Detection of objects in a static image leads to significant improvement in numerous applications such as pedestrian detection, vehicle detection and surveillance (Aslantas and Kurban, 2009; Broggiet al., 2009; Chang, 2010). Several approaches have been invented to detect, identify, classify and tracking objects in stills and videos (Dalal and Triggs, 2005; Dalal, Triggs and Schmid, 2006; Daneshvar and Ghassemian, 2010; Doshiet al.,2012). But still it is highly difficult to discover the objects because of the appearance of noises in the input images. Images acquired by visual sensors are often contaminated by smoke, clouds and bad light condition particularly in the application development includes military and surveillance. For example, detection of foot passengers in the municipal area on the avenue or on campus over night-time results artifacts in visual image because of low light condition. Due to such kind of artifacts appearing in the image, significant features of the relevant objects can hide in the visual image. Human eyes cannot perceive the signals captured by either thermal sensors or night time sensors. Another option, the infrared spectrum that yields imagery based upon the heat content of the scene. As such, it provides a 24 hour imaging capability. So, visual sensors are demanded to dosome tasks noticed to the human eyes. But, some limitations may exist while the individual sensorsare used particularly their cost and maintenance. Temperature that can present as warm blot in IR images is breaded by conveyances. These background noises can make IR-based object detection more complicated. Town views usually have man-made things in their background. For example buildings and street lights whose heat commonly uplift in nightfall. However the utilization of image fusion benefits an alternate to overcome the above limitations. Image fusion is a progress of consolidating information out of more than one image into a single compound image. The fused image yields more information than the original images. The scope of fusion is to make

* Ph.D Research Scholar, Department of Computer Science, Erode Arts and Science College, Erode, Tamil Nadu, India.
Email: reachme.raja@gmail.com

appropriate information from more than one images of a same scene and put up into one single image. Many algorithms have been developed to improve the quality of fusion. PCA, HIS colour model, Brovey, pyramids and Multiscale Geometrical Analysis are most popular fusion methods (Goshtasby and Nikolov, 2007; Haghighat et al., 2011; Han and Bhanu, 2007; Hu and Li, 2012). Generally, Algorithms generated to the fusion of images would lie under pixel-level, feature-level and decision-level (Han and Bhanu, 2007; Hu and Li, 2011; Krebs et al.,1998; Lagendijk et al.,1988; Liet al.,1995) categories.

Multisensor image fusion is yet another popular mechanism in which information from different sensors or modalities are being fused to provide useful complementary information (Li, Cai, and Tan, 2006; Liet al., 2012; Lin and Shi,1999). It plays a vital role in object detection applications which include vehicle safety, night vision, military and medical (Liet al., 2006; Malviya and Bhirud, 2010; Matsopoulos and Marshall,1995; Mikolajczyk et al., 2004). The military systems perform fusion among various sensors such as visual, infrared, radar, passive electronic support measures (ESM) and electro-optic image sensors to specific applications including ocean surveillance, target acquisition, battle-field intelligence and strategic warning, and defense (Mikolajczyk et al., 2004). Similarly, CT, PET, X-Ray, CRT and MRI scan images are carried out to provide the best clinical diagnosis in medical imaging application. Even though CT and MRI are good selections to study bone and hard tissue, it is insufficient to acquire both bone and tissue information at the same time. But fusing both can acquire useful information (Mikolajczyket al.,2004). It can draw the data features of selected sensors to shape a homogeneous image and then dispatch them to the judgment.

Images sensed by different sensors are normally spoiled by noise due to various factors (Muller and Narayanan, 2009). Making a signal noise-free is a notable assignment in image processing (Paris et al., 2008; Piella, 2003). De-noising a noisy image is a broad domain in image restoration. Many techniques have widely been used to restore noisy-free images from noisy images in the literature. Enormous filtering techniques and filters contribute in improving the quality of de-noisy images. The standard of the filters are determined by the robustness in finding crucial details like texture and edges. Due to lack of finding such essential features, it may lead to failure for many filters. Author found very less articles (Riley and Smith, 2006; Siddiquiet al., 2010) in this connection of finding hidden objects using image fusion and bilateral filter particularly in noise images. These articles give more importance to multi-scale bilateral fusion. Obviously, research has to be made on the proper utilization of bilateral filter to image fusion. The aim of this article is to obtain the performance evaluation on, the association of multisensor image fusion and bilateral filter, in terms of discovering hidden objects in noisy visual images. The second section depicts the functionalities of bilateral filter and explains the way to preserve edges during image smoothing. The third section presents the four proposed multi-sensory fusion algorithms using bilateral filter. The last section analyzes the outcomes and pros and cons of the four algorithms.

Bilateral Filter

The procedure of smoothing is one of the momentous assignments in pre-processing step of image processing. Gaussian filtering is the most demotic technique to smooth an image. The concept behind the Gaussian filtering is that intensity value schange slowly over distances. When regarding edges in the image, this idea does not operate well. Naturally, it mis-carries at edges. To defeat this issue, bilateral filter was evolved (Simone et al., 2002) by Tomasi and Manduchi in 1998.

Bilateral filtering denotes as a union of domain and range filtering, non-lineal, non-recurring and local technique. It can conserve edges whereas smooth out images, to express a non-linear uniting of close pixel values (Sochenet al.,1998). In this access, the pixel cost of a location p(x, y) is superseded by average of analogous and close pixel values. It protects edges in a well-fashion manner with the assistance of range filters though smoothing an image. Resulting from its edge preserving properties, it is broadly exploited in many applications (Sun et al.,2006). Though the behaviour of bilateral filter is identicalas Gaussian filter, the weighted average is estimated by both euclidean length and range variance to attain the closed values which is used to replace the center pixel value in the convolution process. Technically, the euclidean length is fixed through spatial domain and the range variance or intensity difference is set through range domain.

The process of finding Euclidean distance is performed in the spatial domain. Consider a vector consists of nearby pixels locations of center pixel. The average weight is calculated to sum up the distance values performed from the vector. The domain filter is given by the equation

$$h(x) = \frac{1}{k_d} \int_{-\alpha}^{\alpha}\int_{-\alpha}^{\alpha} f(\xi)c(\xi,x)\,d\xi \qquad (1)$$

In the above equation, f and h are input and output images which indicates multiband in nature. The center pixel x and nearby point in this filter represents the geometric closeness of the signal. Geometric closeness refers to the value found by Euclidean distance (Simoneet al.,2002). The equation to preserving the DC component for low-pass filtering is defined by

$$k_d(x) = \int_{-\alpha}^{\alpha}\int_{-\alpha}^{\alpha} c(\xi,x)\,d\xi \qquad (2)$$

where, kd is a normalization constant. The procedure $c(\xi, x)$ obtains the geometric difference between the central and nearby pixel. Similarly the function f(x) offers the range filter and is constructed by

$$h(x) = \frac{1}{k_r} \int_{-\alpha}^{\alpha}\int_{-\alpha}^{\alpha} f(\xi)s(f(\xi), f(x))\,d\xi \qquad (3)$$

The pixel similarity between center and nearby pixels is computed by the function s(f(ξ), f(x)). The photometric similarity is calculated by performing the sum of difference from center to nearby intensity values (Simoneet al.,2002). Thus is operated by the range function and c is operated by the domain function. The normalization constant is replaced by

$$k_r(x) = \int_{-\alpha}^{\alpha}\int_{-\alpha}^{\alpha} s(f(\xi), f(x))\,d\xi \qquad (4)$$

Now both the domain and range filter is available to combine and is described by

$$h(x) = \frac{1}{k(x)} \int_{-\alpha}^{\alpha}\int_{-\alpha}^{\alpha} f(\xi)c(\xi,x)s(f(\xi)f(x))\,d\xi \qquad (5)$$

The new value calculated by averaging similar and nearby pixel values would have been placed at the location x. This is what happening while combining the domain and range filters that can be used to achieve bilateral filter to present securing edges while smooth out the image.

$$k(x) = \int_{-\alpha}^{\alpha}\int_{-\alpha}^{\alpha} c(\xi,x)s(f(\xi)f(x))\,d\xi \qquad (6)$$

The mathematical equation (6) represents the convolution operation. The bilateral filter associates low-pass filter and edge stopping function to acquire which attenuates mask weights when it gets high variation among pixel values. The parameters c and s contributes in fixing weights in spatial and range domains. Both are under the control of standard deviations k and r computed in spatial and range domains respectively.

Multisensor Image Fusion using Bilateral Filter

The validity of any research depends upon the systematic approach in conducting the experiment and arriving results based on the output of the experiment. The present study was conducted by identifying objects and input of the image has been first smoothed and then fusion was take place to get the output. Typically, filtering would be done prior to fusion (Teot, 1989; Toet and Walraven, 1996; Toet and Franken, 2003). This method of algorithm was named as Forward Fusion (FF) method.

Figure 1: Forward Fusion

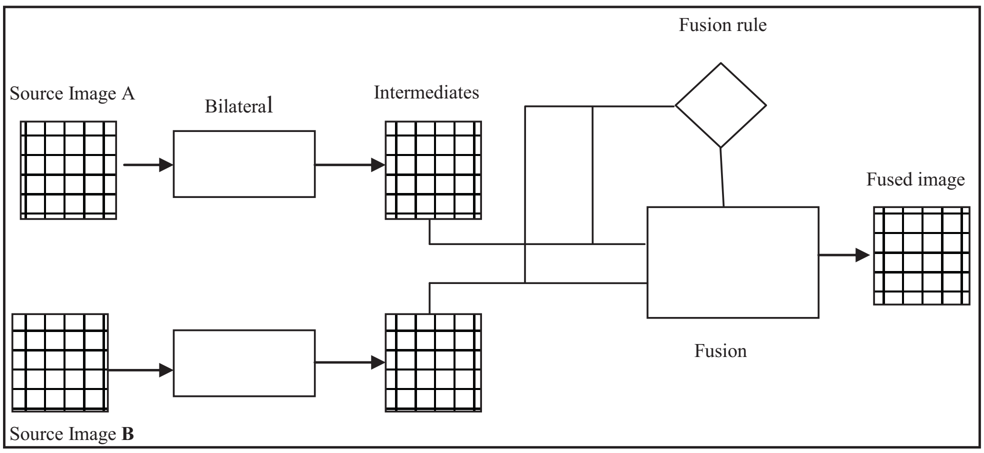

Figure 2: Backward Fusion

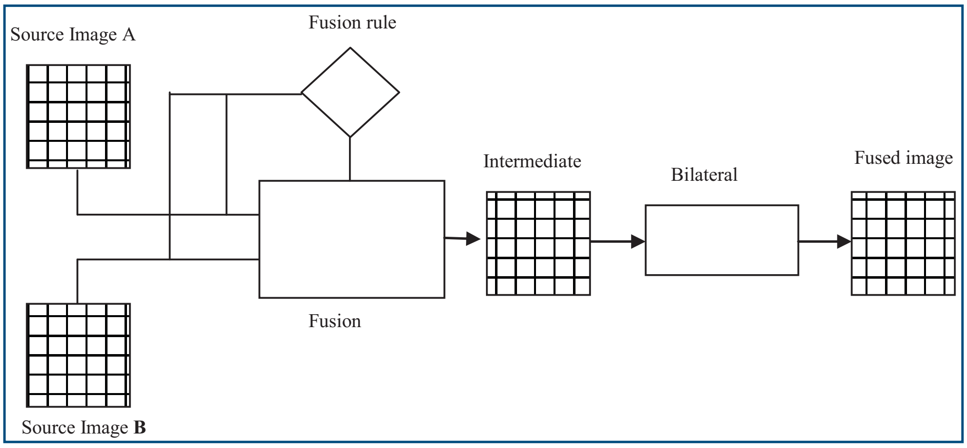

Similarly the same concept has been put in experiment in the reverse form of selecting the input fusion would have been placed first and it is followed by smoothing to get the output. This algorithm was labeled as Backward Fusion (BF). The motivation of this approach is gained from (Toetet al.,2010). In this paper, the fusion would first take place by comparing the sharpen values of adjacent blocks from source noise images which are divided into equally sized blocks. Then a high frequency selective weighted median filter was used to remove isolated blocks in the fused image. Based on these methodologies, we have made an attempt to develop various levels of image fusion algorithms namely Average-Bilateral-Forward-Fusion (ABFF), Average-Bilateral-Backward-Fusion (ABBF), Condition-Bilateral-Forward-Fusion (CBFF) and Condition-Bilateral-Backward-Fusion (CBBF) to achieve the retrieval of hidden objects. Our MIBL (Multisensor Imagefusion using Bilateral Filter) consists of four fusion algorithms derived from the former described ideas FF and BF. The need of this attempt is to show the impact of both techniques and abilities to discovering significant objects from noisy multisensor imaging.

Figure 1 and 2 depict an elaborate plan of this work. The Figure s show that the process is classified into two folds. In FF, the process begins by filter and end with fusion establishes in Figure 1. In contrary, Figure 2 describes fusion begins first and filter last. This work describes in two parts namely fusion and filter. The filter part is adjustable to the fusion part that can be fixed either before or after the fusion. The following sections explain algorithms for the fusion of multi-sensor images using FF and BF.

In this portion, we will describe the proposed algorithms which show the clear picture about the combining techniques to obtain noise-less fused image with clear recovered targets. The root images are supposed to be registered to produce a more instructive fused image.

Average-Bilateral-Forward-Fusion

The fusion procedure of (ABFF) is described as follows: The algorithm ABFF is comprised into two folds. The first portion is the process of eliminating noise from the corrupted images. Immediately after that, the de-noised pixels are step in to the second portion, where the average merging of two consecutive pixels would be computed. Firstly, the sources A and B are smoothed by the bilateral filter to obtain the respective IR and Visual de- noise images. The smoothing part contains the following steps. The Gaussian distance weights need to be calculated in the spatial domain that is represented by

$$p = \sum \sum e^{\frac{\left(X^2+Y^2\right)}{2\sigma_d^2}} \tag{7}$$

where G provides the value of Pre-computed Gaussian Distance (PGD) weights. X and Y give the distance from the origin in horizontal and vertical axis respectively. σ presents standard deviation of the Gaussian distribution. Each pixel is assigned as a new value by a weighted average of that pixel's neighborhood. The highest weight is set to the original pixel and smaller weights are assigned to the neighboring pixels as their distance to the original pixel increases. To compute Gaussian intensity weights

$$q = \sum \sum e^{\frac{(I-A(i,j))^2}{2\sigma_r^2}} \quad (8)$$

It is important step to find out the minimum, maximum and range pixel values based on the filter size prior to form the mask in the range domain. The amazing smooth results would be attained by associating both domain and range filters. It is given in Figure 3 in which, the variable I extracts the local region value in finding minimum and maximum range value according to the size of window. The Gaussian intensity weights derived from the range values is given by the variable q. The given procedure is used to calculate bilateral filter response.

$$f = \sum_n p(\|m-n\|)\, q(\|w_m - w_n\|)\, w_n \quad (9)$$

In second part, according to the given fusion rule, the smoothed IR and Visual images are getting fused respectively to obtain the fused images F. Here the rules taken to the fusion is average fusion by calculating the average pixel values IR and visual pixels from respective position.

$$F(i,j) = \frac{(V(i,j) + I(i,j))}{2} \quad (10)$$

The algorithm given in Figure 3 is explained only for ABFF and CBFF. The remaining algorithms originated from Figure 3 can be obtained by replacing step 4 with step 2. So, the process begins from fusion and end to smoothing.

Average-Bilateral-Backward-Fusion (ABBF)

The second one can be in inverse sequence of the ABFF algorithm. First of all, the average – pixel fusion is executed for all the pixels in Visual and IR using equation (9). So, obviously the filter is settled in rearward situation. The outcome perverted by noise can be the result. Then the fused image is forwarded to the series of actions includes PGD for calculating Gaussian distance weight, ELRV for extracting local region, GIV for computing Gaussian intensity weight and GFR for performing the replication of Gaussian filter. Ultimately, the fused-noisy image is transformed into de-noised fusion image.

Condition-Bilateral-Forward-Fusion(CBFF)

The previous algorithm can be modernized by shifting conditional rule in fusion portion to make superior fulfillment for various applications (related to different applications). We have restored the algorithm by appending the conditional fusion in place of average fusion. The conditional fusion can be played as MAX_CHOOSE orMIN_CHOOSE rules based on the application requirement. First smooth can be carried out on both images by the sequence of steps contains calculating Gaussian distance weight, extracting local region, computing Gaussian intensity weight and performing the response of Gaussian filter. Either MAX_CHOOSEor MIN_CHOOSE executes the smoothed images to produce the final fused image using the equations given below.

$$F(i,j) = \begin{cases} f_{vi}(i,j) if |f_{vi}(i,j)| > |f_{ir}(i,j)| \\ f_{ir}(i,j) else \end{cases} \quad (11)$$

(or)

$$F(i,j) = \begin{cases} f_{vi}(i,j) if |f_{vi}(i,j)| < |f_{ir}(i,j)| \\ f_{ir}(i,j) else \end{cases} \quad (12)$$

Condition-Bilateral-Backward-Fusion(CBBF)

In CBBF, conditional fusion can be applied on IR and visual images. According to the fusion rule either MAX-CHOOSE or MIN-CHOOSE is elected to carry out fusion of origin images. The fused image can be implicated to procure Gaussian distance weight. The local region values can be extracted. At last, Gaussian intensity and Gaussian filter response must be computed.

Figure 3: The Pseudo Code of ABFF

Input: N source images, standard deviations σ_r and σ_d

Output : the fused image F

Step 1:

Read noisy IR and Visual image pixel values

Step 2:

Apply pre-compute Gaussian distance weights

Perform $p = e^{x^2+y^2/2\sigma_d^2}$

Step 3.

For each pixel in the position (x, y)

Begin

Compute $I = A(xMin : xMax, yMin : yMax)$

Compute $q = e^{(-(I-A(x,y)))^2/2\sigma_r^2}$

$$\text{Compute } f = q * p((xLow : xHigh) - x + w + 1, (yLow : yHigh) - y + w + 1)$$

End

Step 4:

For each pixel in the position (x, y) IR and Visual images

Begin

$$\text{Compute } F = (f_{vi} + f_{ir})/2$$

(or)

$$\text{Compute } F(x,y) = \begin{cases} f_{vi}(x,y) if |f_{vi}(x,y)| > |f_{ir}(x,y)| else \\ f_{ir}(x,y) \end{cases}$$

(or)

$$\text{Compute } F(x,y) = \begin{cases} f_{vi}(x,y) if |f_{vi}(x,y)| < |f_{ir}(x,y)| else \\ f_{ir}(x,y) \end{cases}$$

end

Experimental Results and Discussions

Some scenarios describe that the practical improvement is befall in the procedure of fusion at the time of detecting targets. It is very difficult to detect the target when the foreground and background objects are possessing same colour and intensity values. It is really challenging when the objects are not visible clearly in night time including vehicles on the road with head-lamp and objects beyond lighting lamp. To overcome these difficulties, four algorithms are examined with four sets of visual and IR images downloaded from www.imagefusion.org.

We hired a bilateral fusion design to generate a range of fused images to be employed as input to the disclosure of hidden objects. Altogether four couple of multisensor (visual and IR) images were carried out to investigate the recommended algorithms. Figure 4 shows that the images corrupted by Gaussian noises are randomly claimed to get the strength of bilateral filter. To assess the performance of proposed ways, three quality metrics such as entropy, mean and standard deviationare utilized.

Entropy:

Entropy is a statistic quality metric applied to survey the quantity of information live in the image (Krebset al.,1998). It grants the average information volume of an image. The rate of entropy must be higher than the parent image shows that the result image has more information (Tomasi and Manduchi, 1998). Entropy is computed as

$$H = -\sum p(i)\log_2(p(d_i)) \tag{13}$$

G- Gray levels; p(di) – Probability of occurrence of a particular gray level di. .

Standard Deviation:

The contrast of the fused image is calculated by Standard deviation (Toetet al., 2010). A high contrast image must have high standard deviation.

$$\sigma = \sqrt{\sum_{i=0}^{L}(i - \bar{i})^2 h_{I_f}} \tag{14}$$

L – Number of repeated intensity in a signal: lf – combinedsignal: hlf – normalized histogram of mergedimage (Xuet al., 2005).

Figure 4: Visual (First Row) and IR (Second Row) Noisy Images of Uncamp, Pedestrian, Seashore and Traffic

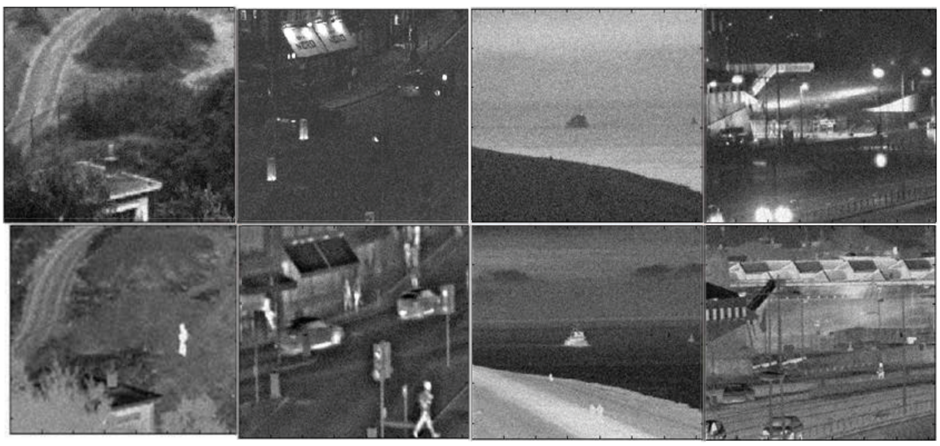

Figure 5: Fusion and Noise Removal of Uncamp Image by ABFF, ABBF, CBFF and CBBF

Relative Mean

Relative mean is used to find out the central value of the distribution of the pixels in that band. The relative shift mean is defined as

$$rm = \frac{\mu_f - \mu_r}{\mu_r} x100 \qquad (15)$$

The first trail is directed on the "uncamp" visible and IR images. In the first row of Figure 4, the person in the scene is displayed clearly in IR image butmissing in the visual image. The resulted images, shown in Figure 5, are the issues of the proposed ABFF, ABBF, CBBF and CBFF algorithms. The outcome of first two approaches (ABFF and ABBF) are depressingly dark than other two. Since the intensity of object is small, it is quite heavy to discriminate the background and foreground. Tables 1 and 2 submit the quantitative results of performance evaluation of the proposed algorithms. Based on the quantitative metric, the best result is obtained in CBFF and CBBF algorithms. The conditional forward algorithms reach the best result through the estimation evaluated by the metrics entropy, mean and standard deviation. The CBFF reaches 6.6777, 0.4394, 0.1142 meanwhile the second best result is achieved by CBBF over the assess 6.5826, 0.448, 0.1110. On the whole, the conditional forward method shows the best result for uncamp images based on quantitative result as well as brighter human object than the background.

Next, the second attempt is encountered on "pedestrian images". Since the visual image was taken in night, the objects such as road, signals and pedestrians crossing the road are not capable of being perceived in visual image. Because of the heat emitting sense of the objects, the IR image represent those objects. Figure 6 shows noisy images and resulted images of four proposed algorithms. Based on the results obtained by the proposed algorithms, subjectively, the objects recovered in average fusion implies slightly darker than conditional procedures. This attribute may lead some difficulties in further process like improper segmentation and classification. Because, the forefront objects are very near to background. The conditional forward and backward algorithms present best performance based on visual and numerical quantitative analysis. Inquantitative performance, the entropy and SD values are high in condition forward and the mean value is high in conditional backward. For the metric entropy, CBFF reaches 6.7062, the second best one is 6.6834 obtained by CBBF. Similarly, the CBFF present best result 0.1142 for the metric STD than the second best 0.1110 presented by CBBF.

Figure 6: Fusion and Noise Removal of Pedestrian Image by ABFF, ABBF, CBFF and CBBF

Figure 7: Fusion and Noise Removal of Seashore Image by ABFF, ABBF, CBFF and CBBF

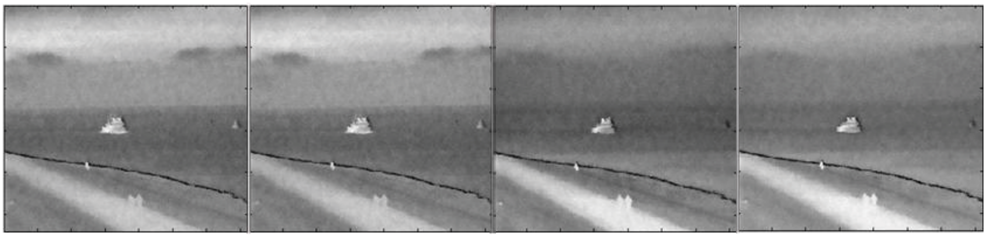

The third experiment is performed over "seashore" images. The noise-free fused image offers the best environment for target detection. The objects including a ship on the sea, persons walking on the seashore would be visible clearly in the resulted images and is shown in Figure 7. But the challenge begins when a couple of persons are considered. Because both background and foreground objects are emerging in same colour and intensity. Among the four proposed methods, the CBFF algorithm gives good numerical results like 6.1085, 0.5608 and 0.0793 for the metrics entropy, mean and standard deviation respectively. In the subject testing, the possibility of consideration goes to ABFF and ABBF in detecting small and dim targets. Naturally, a small boat appearing in the right side would get clear observation from the resulted images of ABFF and ABBF.

The fourth experiment is conducted over "traffic "images. The process of illumination-removal plays an essential role in recovering hidden objects from visual images. In this scenario, two objects were taken for experiments. One is car with shining headlight and another one is person standing behind the light lamp. Both are concealed due to the illumination of light condition in visual image. But these objects are displayed in IR images.

The experimental results show that the numerical results 7.1831 for entropy, 0.1618 for SD in CBFF and 0.4697 for mean in CBBF.

Recovering objects in such conditions matters a lot. CBFF has done well at recovering things in those conditions. The person behind the light spot in pedestrian image is discovered almost 75% in CBFF algorithm using $AF(i,j) = \begin{cases} V(i,j) if \, |v(i,j)| < |i(i,j)| \\ I(i,j) else \end{cases}$ rule.

Figure 8 illustrates the recovered clear image of the car and person behind the hotspot.

Figure 8: Fusion and Noise Removal of Traffic Image by ABFF, ABBF, CBFF and CBBF

Figure 9: Person Restored From Hotspot Using CBFF with MIN-CHOOSE Algorithm

Table 1: Quantitative Assessment of ABFF and ABBF

Images	*ABFF*			*ABBF*		
	Entropy	*Mean*	*SD*	*Entropy*	*Mean*	*SD*
Un-camp	6.1822	0.3572	0.0866	6.1281	0.3571	0.0849
pedestrian	5.8616	0.2038	0.0783	5.8003	0.2045	0.0748
seashore	5.7416	0.4210	0.0568	5.6493	0.4210	0.0554
traffic	6.7774	0.3790	0.1164	6.7445	0.3790	0.1133

Table 2: Quantitative Assessment of CBFF and CBBF

Images	*CBFF*			*CBBF*		
	Entropy	*Mean*	*SD*	*Entropy*	*Mean*	*SD*
Uncamp	6.6777	0.4394	0.1142	6.5826	0.4448	0.1110
Pedestrian	6.7062	0.3282	0.1345	6.6834	0.3288	0.1333
Seashore	6.1085	0.5608	0.0793	6.0873	0.5606	0.0774
Traffic	7.1831	0.4641	0.1618	7.1423	0.4697	0.1586

Conclusion

In this paper, an attempt has been made to bring out the research for the association of bilateral filter and image fusion in order to detect the hidden object in the visual scene. In this connection, different ways had been depicted in utilization of the both procedures which can carry out further research in future. The proposed Average-Forward, Average-Backward, Conditional-Forward and Conditional-Backward algorithms of multisensor image fusion technique are discussed. They were applied to discover hidden objects by fusing IR and Visual images using bilateral filter. They makes possible to find out objects having worst background like smoke, illumination and bad whether climate. Recovering objects in such conditions matters a lot. CBFF with MIN-COOSE rule has done well at recovering things in those conditions. According to the qualitative result, we concluded that conditional forward algorithms are suited for disclosing the hidden objects. The future work will be forwarded to restore the objects behind the shining hotspot and smoke.

References

Aslantas, V. & Kurban, R. (2009). A comparison of criterion functions for fusion of multi-focus noisy images. *Optics Communication*, 282(16), 3231-3242.

Broggi, A., Cerri, P., Ghidoni, S., Grisleri, P. & Gi, H. (2009). *A New Approach to Urban Pedestrian Detection for Automatic Braking*. IEEE Transactions on Intelligent Transportation Systems, 10(4), 594-605.

Chang, H. (2010). *Entropy-based Trilateral Filtering for Noise Removal in Digital Images*. 2010 3rd International Congress on Image and Signal Processing (CISP2010), 2, 673-677.

Dalal, N. & Triggs, B. (2005). *Histograms of Oriented Gradients for Human Detection*. IEEE Computer Society Conference on Computer Vision and Pattern Recognition, 1, 886-893.

Dalal, N., Triggs, B. & Schmid, C. (2006). *Human Detection using Oriented Histograms of Floe and Appearance*. Proceedings of the 9th European Conference on Computer Vision, Part II, 428-441.

Daneshvar, S. & Ghassemian, H. (2010). MRI and PET image fusion by combining IHS and retina-inspired models. *Information Fusion*, 11(2), 114-123.

Doshi, N. P., Schaefer, G. & Merla, A. (2012). *An Evaluation of Image Enhancement Techniques for Capillary Imaging*. Proceedings of the IEEE International Conference on System, Man and Cybernetics (SMC), 1428-1432.

Goshtasby, A. A. & Nikolov, S. (2007). Image fusion: Advances in the state of the art. *Information Fusion*, 8(2), 114-118.

Haghighat, M. B. A., Aghagolzadeh, A. & Seyedarabi, H. (2011). A non-reference image fusion metric based on mutual information of image features. *Computers and Electrical Engineering*, 37(5), 744-756.

Han, J. & Bhanu, B. (2007). Fusion of color and infrared video for moving human detection. *Pattern Recognition*, 40(6), 1771-1784.

Hu, J. & Li, S. (2012). The multi-scale directional bilateral filter and its application to multisensory image fusion. *Information Fusion*, 13(3), 196-206.

Hu, J. & Li, S. (2011). *Fusion of Panchromatic and Multispectral Images Using Multi-Scale Dual Bilateral Filter*. 18th IEEE International Conference on Image Processing (ICIP), (pp. 1489-1492).

Krebs, W. K., Scribner, D. A., Miller, G. M., Ogawa, J. S. & Schuler, J. (1998). *Sensor Fusion: Architectures, Algorithms, and Applications II*. SPIE - International Society for Optical Engineering, 2, 129-140. Bellingham, WA.

Lagendijk, R. L., Biemond, J. & Boekee, D. E. (1988). *Regularized Iterative Image Restoration with Ringing Reduction*. IEEE Transactions on Acoustics, Speech and Signal Processing, 36(12), 1874-1887.

Li, H., Manjunath, S. & Mitra, S. (1995). Multi-sensor image fusion using the wavelet transform. *Graphical Models and Image Processing*, 57(3), 235-245.

Li, M., Cai, W. & Tan, Z. (2006). A region-based multi-sensor image fusion scheme using pulse-coupled neural network. *Pattern Recognition Letters*, 27(16), 1948-1956,

Li, H., Chai, Y., Yin, H. & Liu, G. (2012). Multi-focus image fusion and de-noising scheme based on homogeneity similarity. *Optics Communications*, 285(2), 91-100.

Lin, Z. & Shi, Q. (1999). *An Anisotropic Diffusion PDE for Noise Reduction and Thin Edge Preservation*. Proceedings of the 10th International Conference on Image Analysis and Processing. (pp. 102-107).

Malviya, A. & Bhirud, S. G. (2010). Visual infrared video fusion for night vision using background estimation. *Journal of Computing*, 2(4), 66-69.

Matsopoulos, G. K. & Marshall, S. (1995). Application of morphological pyramids: Fusion of MR & CT phantoms. *Journal of Visual Communication and Image Representations*, 6(2), 196-207.

Mikolajczyk, K., Schmid, C. & Zisserman, A. (2004). *Human Detection based on Probabilistic Assembly of Robust Part Detectors*. European Conference on Computer Vision, Lecturer notes in Computer Science, 3021, 69-82.

Muller, A. C. & Narayanan, S. (2009). Cognitively-engineered multi-sensor image fusion for military applications. *Information Fusion*, 10(2), 137-149.

Paris, S., Kornprobst, P., Tumblin, J. & Durand, F. (2008). Bilateral Filtering: Theory and Applications. *Foundations and Trends in Computer Graphics and Vision*, 4(1), 1-73.

Piella, G. (2003). A general framework for multi-resolution image fusion: From pixels to regions. *Information Fusion*, 4(4), 259-280.

Riley, T. & Smith, M. (2006). *Image Fusion Technology for Security and Surveillance Applications*. Proceedings of SPIE 6402, Optics and Photonics for Counterterrorism and Crime Fighting II, 6402.

Siddiqui, A. B., Jaffar, M. A., Hussain, A. & Mirza, A. M. (2010). *Block-based Feature-level Multi-focus Image Fusion*. 5th International Conference on Future Information Technology.

Simone, G., Farina, A., Morabito, F. C., Serpico, S. B. & Bruzzone, L. (2002). Image fusion techniques for remote sensing applications. *Information Fusion*, 3(1), 3-15.

Sochen, N., Kimmel, R. & Malladi, R. (1998). *A Geometrical Framework for Low Level Vision*. IEEE Transactions on Image Processing, 7(3), 310-318.

Sun, Z. H., Bebis, G. & Miler, R. (2006). *On-Road Vehicle Detection: A Review*. IEEE Transactions on Pattern Analysis and Machine Intelligence, 28(5), 694-710.

Teot, A. (1989). Image fusion by a ratio of low-pass pyramid. *Pattern Recognition Letters*, 9, 245-253.

Toet, A. & Walraven, J. (1996). New false color mapping for image fusion. *Optical Engineering*, 35(3), 650-658.

Toet, A. & Franken, M. (2003). Perceptual evaluation of different image fusion schemes, *Displays*, 24(1), 25-37.

Toet, A., Hogervorst, M. A., Nikolov, S. G., Lewis, J. J., Dixon, T. D., & Bull, D. R. (2010). Towards cognitive image fusion. *Information Fusion*, 11(2), 95-113.

Tomasi, C. & Manduchi, R. (1998). Bilateral Filtering for Gray and Color Images. 6th IEEE *International Conference on Computer Vision*. (pp. 839-846).

Xu, F., Liu, X. & Fujimura, K. (2005). *Pedestrian Detection and Tracking with Night Vision*. IEEE Transactions on Intelligent Transportation Systems, 6(4), 63-71.